scientific reports

Check for updates

OPEN

Role of hypertrophic adipocytes, collagen VI, and CD38 in adipose tissue fibrosis in obesity

Angelica Di Vincenzo[1,21], Tonia Luca[2,21], Jessica Perugini[1], Giovanni Lezoche[3], Vincenza Barresi[4], Vincenzo De Geronimo[5], Abele Donati[6], Erika Casarotta[6], Mario Tomasello[7], Salvatore Pezzino[8], Chiara Scuderi[4], Adriano Di Cristoforo[9], Alessio Pieroni[10], Massimiliano Petrelli[10], Maria Vittoria Napoli[11,12], Nayra Figueiredo[13], Flavia Campos Corgosinho[13], Andrea Sbarbati[14], Luciano Merlini[15], Patrizia Sabatelli[16], Laura Graciotti[17], Tatiana Spadoni[17], Christian Dani[18], Monica Mattioli-Belmonte[19], Daniele Filippo Condorelli[4], Armando Gabrielli[11,12], Fabio Malavasi[20], Antonio Giordano[1], Sergio Castorina[2,7] & Saverio Cinti[1]✉

Adipose tissue fibrosis is associated with metabolic alterations in patients with obesity and involves three major collagen types: fibrillar collagens I and III and non-fibrillar collagen VI. In this study, fibrosis was found to be significantly increased only in visceral adipose tissue in patients with obesity (4.7% vs. 2.5% in controls, $p < 0.001$), whereas no significant difference was observed in subcutaneous adipose tissue. Transmission electron microscopy and high-resolution scanning electron microscopy suggested that hypertrophic adipocytes may contribute to the production of fibrillar collagens I and III. In vitro data were consistent with this interpretation. Expression of the *COL6* gene, which encodes the non-fibrillar collagen VI, was reduced in adipose tissue from obese patients. Notably, patients carrying mutations in *COL6* genes displayed increased fibrosis even in subcutaneous fat, approximately 6.5-fold higher than controls in the patient with the severe form (Ullrich) and 2.8-fold higher in two patients with the milder form (Bethlem). Approximately 15% of adipocytes in obese tissue appeared stressed or dead (perilipin-1 negative), and the associated infiltrating macrophages exhibited increased expression of CD38, an ectoenzyme implicated in systemic fibrosis. Correlations with gene expression also indicated the importance of myofibroblasts and the extracellular-matrix peptidase D. Taken together,

our data suggest that obese adipocytes may contribute to fibrillar collagen production and identify collagen VI and CD38 as potential molecular contributors, consistent with the concept that adipose tissue fibrosis in humans has a multifactorial origin.

Keywords Obesity, Adipose tissue fibrosis, Visceral fat, COL6, CD38, Pathogenesis

[1]Center for the Study of Obesity, Department of Experimental and Clinical Medicine, Marche Polytechnic University, Via Tronto 10a, Ancona 60126, Italy. [2]Department of Medical, Surgical Sciences and Advanced Technologies G.F. Ingrassia, University of Catania, Via Santa Sofia, 87, Catania 95123, Italy. [3]Department of Experimental and Clinical Medicine, Section of Surgical Sciences, Marche Polytechnic University, Via Tronto 10a, Ancona 60126, Italy. [4]Department of Biomedical and Biotechnological Sciences, Section of Medical Biochemistry, University of Catania, Via Santa Sofia 89, Catania 95123, Italy. [5]Unit of Endocrinology, Policlinico Morgagni CCD, Catania 95125, Italy. [6]Anesthesia and Intensive Care Unit, Department of Biomedical Sciences and Public Health, Marche Polytechnic University, Via Tronto 10a, Ancona 60126, Italy. [7]Mediterranean Foundation "G.B. Morgagni", Catania, Italy. [8]Department of Medicine and Surgery, Kore University of Enna, Contrada Santa Panasia, Enna 94100, Italy. [9]Department of Science and Engineering of Matter, Environment and Urban Planning, Via Brecce Bianche 12, Ancona 60131, Italy. [10]Clinic of Endocrinology and Metabolic Diseases, Marche Polytechnic University, Via Tronto 10a, Ancona 60126, Italy. [11]Foundation of Molecular Medicine and Cellular Therapy, Marche Polytechnic University, Via Tronto 10a, Ancona 60126, Italy. [12]Hiller Research Center, University Hospital Düsseldorf, Medical Faculty of Heinrich Heine University, Düsseldorf, Germany. [13]Postgraduate Program in Health Sciences, Faculty of Medicine, Federal University of Goiás (UFG), 5th Avenue, s/n - Setor Leste Universitário, Goiânia 74605-050, GO, Brazil. [14]Department of Neuroscience, Biomedicine and Movement Sciences, Strada le Grazie 8, Verona 37134, Italy. [15]Department of Biomedical and Neuromotor Science, University of Bologna, DIBINEM, Bologna 40136, Italy. [16]CNR, Institute of Molecular Genetics "Luigi Luca Cavalli-Sforza", Via di Barbiano 1/10, Bologna 40136, Italy. [17]Center for Confocal, Electron Microscopy and CLEM, Department of Biomedical Science and Public Health, Faculty of Medicine, Marche Polytechnic University, Via Tronto, 10, Ancona 60126, Italy. [18]Faculté de Médecine, CNRS, INSERM, iBV, Université Côte d'Azur, CEDEX 2, Nice F-06107, France. [19]Department of Clinical and Molecular Sciences, Marche Polytechnic University, Via Tronto 10a, Ancona 60126, Italy. [20]Department of Medical Sciences, University of Torino Medical School, Fondazione Ricerca Molinette Ets, Via Valeggio 41, Torino 10129, Italy. [21]Angelica Di Vincenzo and Tonia Luca contributed equally to this work. ✉email: s.cinti@staff.univpm.it

Adipose tissue is a complex organ that has recently been recognized as forming a unitary structure in both mice and humans[1]. In individuals with obesity, the adipose organ is marked by chronic low-grade inflammation and fibrosis[2,3]. While the pathogenesis and clinical consequences of chronic inflammation are well understood, the role of fibrosis remains less clear and is still a matter of debate. Nonetheless, several studies have linked visceral fat fibrosis to glucose and lipid dysmetabolism[4,5], and other evidence suggests possible oncogenic associations[6].

In obesity, adipose tissue primarily contains three major types of collagen: collagen I, collagen III, and collagen VI[7]. While collagens I and III are mainly associated with the classical mechanical consequences of fibrosis[8–10], the role of collagen VI is more complex and not fully understood[11–14].

Although collagen VI is expressed throughout the body, it is particularly abundant in the extracellular matrix of adipose tissue[7,15], suggesting that it plays a key role in adipose tissue physiology.

Mutations in the *COL6* genes (*COL6A1*, *COL6A2*, and *COL6A3*) cause a group of related myopathies (COL6-RM) characterized by muscle weakness, joint contractures and skin abnormalities. These conditions represent a clinical spectrum ranging from severe early-onset forms (Ullrich Congenital Muscular Dystrophy, UCMD) to milder (Bethlem Myopathy, BM) and intermediate phenotypes[16]. In the EU, a rare disease is defined as one affecting fewer than 5 individuals per 10,000. COL6 myopathies are extremely rare, with estimated prevalences of 0.77 per 100,000 for BM and 0.13 per 100,000 for UCMD, corresponding to a combined prevalence of approximately 1 per 100,000[17].

In this study, we analyzed subcutaneous and visceral (omental) fat biopsies from patients with obesity undergoing bariatric surgery, as well as from lean controls. Morphometric analysis of Sirius Red-stained histological sections revealed significant fibrosis only in visceral fat, consistent with previous findings[3,18,19].

Expression of *COL1A1* and *COL3A1* (the most representative isoforms of *COL1* and *COL3*) was slightly increased in visceral fat, while the expression of *COL6A3* (the most representative isoforms of COL6) was significantly reduced. Electron microscopy (both transmission-TEM and high-resolution scanning microscopy-HRSEM) showed that a fibrillar collagen network is a normal structural component of the adipocyte surface. In obese adipocytes, this fibrillar network appears to be increased, likely because of reduced *COL6* expression, as suggested by gene expression data and in vitro gene-silencing experiments. Furthermore, fat biopsies from patients carrying homozygous (Ullrich) or heterozygous (Bethlem) mutations in the genes for collagen VI showed high levels of fibrosis, exceeding those observed in obesity-associated adipose tissue. These findings indicate an important role for collagen VI in the development of fat fibrosis.

CD38, an ectoenzyme implicated in the pathogenesis of systemic sclerosis, an autoimmune disease characterized by skin and organ fibrosis[20,21], also showed a positive correlation with visceral fat fibrosis, accompanied by macrophage-driven inflammation. Immunohistochemical analysis revealed strong CD38 immunoreactivity in both macrophages and adipocytes within obese adipose tissue, suggesting that CD38 may contribute to fat fibrosis through an additional molecular pathway. However, gene modulation experiments did not demonstrate a direct functional link between *COL6* and *CD38*, suggesting that their roles in fat fibrosis may be independent.

Overall, our findings align with previous studies[3,22–24] in suggesting that fat fibrosis is of multifactorial origin, and indicate that obese adipocytes may represent a source of collagen production. Moreover, our data highlight an unexpected role for both collagen VI and CD38 in the altered metabolic state of obese visceral cells, ultimately contributing to fat fibrosis.

Results

Omental adipose tissue from patients with obesity shows parenchymal fibrosis

Adipocytes from subcutaneous and visceral (omental) fat in patients with obesity (clinical data in Suppl. Table 1) are widely considered hypertrophic[25], and our quantitative data confirm that both visceral and subcutaneous adipocytes are enlarged compared with those of lean controls, with greater hypertrophy observed in subcutaneous than in visceral fat (Suppl. Figure 1).

This finding is consistent with previous data[26]. Notably, only perilipin1 (PLIN1)-positive adipocytes were analyzed to exclude confounding results from dead or unhealthy adipocytes[27–29].

Sirius Red staining and high-resolution scanning electron microscopy (HRSEM) revealed a variable degree of fibrosis, both surrounding groups of adipocytes and encasing single adipocytes (pericellular fibrosis), in line with observations from other studies[3,30](Fig. 1A).

The distribution of fibrosis among patients was highly heterogeneous. When compared with the corresponding fat tissue from lean controls, fibrosis was significantly increased only in omental fat (Fig. 1B). Correlations with lipid metabolic markers (with a similar trend observed for glycemia) further support the clinical relevance of visceral fibrosis, in agreement with previous studies[3–5,19,30,31](Table 1).

A large proportion of hypertrophic adipocytes appeared stressed or dead

Hypoxia resulting from adipocyte hypertrophy is thought to contribute to fibrosis[32,33]. Consistently, the anatomical arrangement of fibrous bundles encasing groups of adipocytes or individual adipocytes may lead to a form of "self-choking", or mechanically induced hypoxia (Fig. 1A).

Hypoxia can cause adipocyte death, and dead adipocytes surrounded by pericellular fibrosis have been described[31], though not previously quantified.

Since PLIN1 is a marker of adipocyte viability[27–29], we measured the percentage of tissue occupied by PLIN1-negative adipocytes. A substantial proportion of subcutaneous (about 15%) and visceral (about 12%) fat from patients with obesity consisted of PLIN1-negative (dead or stressed) adipocytes, compared with only 4% (subcutaneous) and 3% (visceral) in lean controls (Fig. 1D and E). A positive correlation between the proportions of PLIN1-negative adipocytes in subcutaneous and visceral fat was observed in individual patients, suggesting a systemic patient-specific phenomenon (Fig. 1F). The percentage of PLIN1-negative adipocytes in lean patients was consistent with published estimates of physiologic adipocyte turnover in humans[34]. We further observed that many PLIN1-negative adipocytes were located in proximity to fibrotic areas. To explore this relationship, we analyzed the correlation between the extent of fibrosis and the proportion of PLIN1-negative adipocyte areas. A strong positive correlation was found (Fig. 1G), which remained significant even after stratification by gender (Suppl. Figure 2).

These findings suggest that adipocyte stress or death may contribute to the development of adipose tissue fibrosis in patients with obesity.

Obese adipocytes may contribute to fibrosis

TEM and HRSEM showed a fibrillar collagen network on the surface of adipocytes from lean patients, suggesting that it is a normal structural component of adipocyte anatomy, consistent with previous observations in mice[35]. This collagen network appeared thickened and composed of larger fibrils on the surface of obese adipocytes. Furthermore, prominent sprouting of fibrils and microfibrils was frequently observed on the surface of obese adipocytes (Fig. 2A-C, G and H), as previously reported in obese mouse adipose tissue[35].

These findings indicate that adipocytes may be capable of producing collagen fibrils, in keeping with the increased metabolic activity observed in hypertrophic adipocytes[36]. To examine this possibility in human samples, we analyzed electron microscopy images of visceral fat from patients with obesity and fibrosis > 5% (n = 9), comparing them with those from patients with fibrosis < 5% (n = 9) and lean individuals (n = 6). Both TEM and HRSEM pointed to collagen fibril production by adipocytes, with no obvious differences between samples with fibrosis > 5% and those with fibrosis < 5%. However, in visceral fat we also identified a variable number of structurally altered fibrils among those with otherwise normal morphology, mainly types I and III; these were observed predominantly in patients with fibrosis > 5%. Their diameter was approximately twice that of normal type I and III collagen fibrils, and their ultrastructure appeared frayed (Fig. 2D and E). Quantitative data showed that size of type I e and type III collagen fibrils in the adipose tissue of patients with obesity was significantly larger than collagen fibrils found in lean patients. Collagen fibrils of adipose tissue from the patient with Ullrich syndrome (see Sect. 2.8) were not significantly different from that of patients with obesity (Fig. 2F).

Human adipocytes express collagen genes in vitro

Taken together, these findings suggest that at least part of the collagen fibrils contributing to adipose parenchymal fibrosis may be produced directly by adipocytes. To investigate this possibility, we analyzed gene expression in a well-established human adipocyte model: hMADS[37]. Because collagen fibrils are generally thought to be produced primarily by fibroblasts, we compared these data with those obtained from a human dermal fibroblast cell line (NhDF)[38].

Differentiated hMADS cells, corresponding to mature adipocytes, expressed levels of *COL1A1* at levels comparable to those observed in fibroblasts, but showed higher expression of *COL3A1* and *COL6A3* than NhDF cells (Fig. 3A).

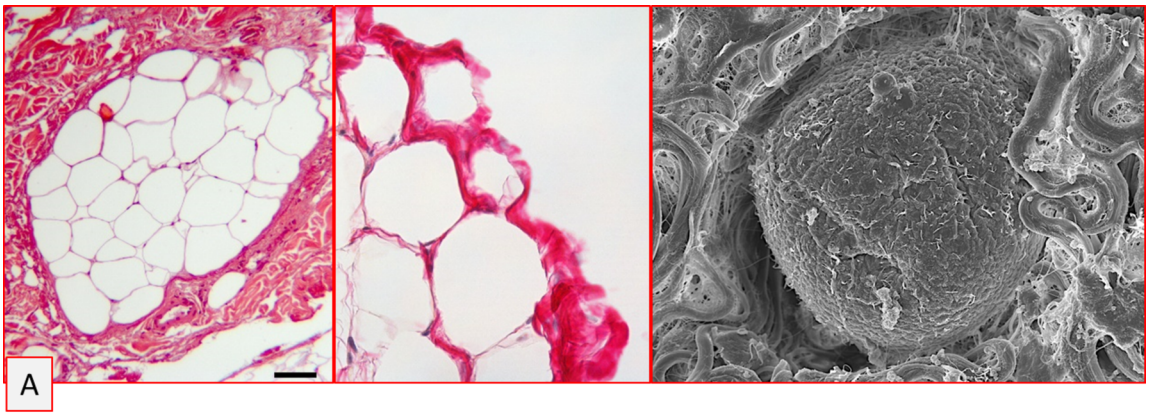

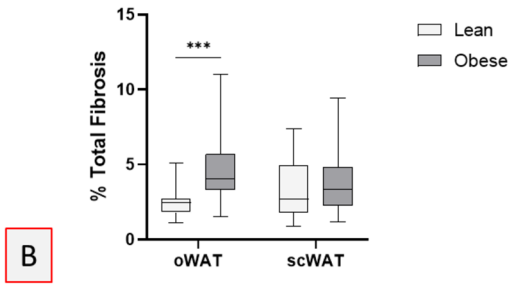

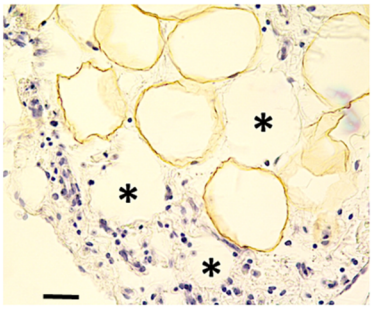

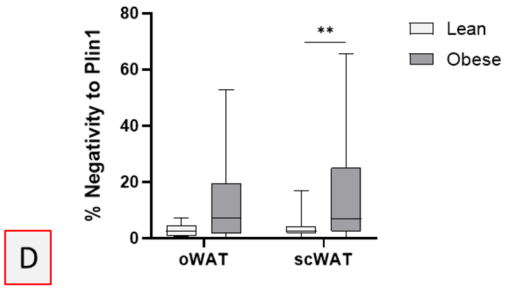

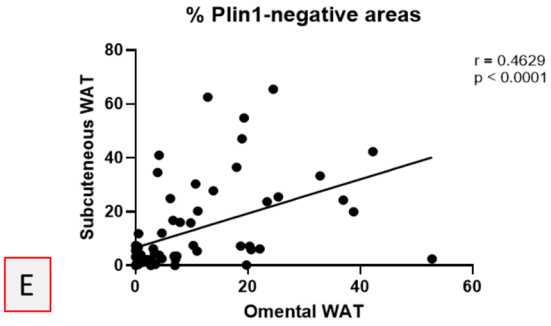

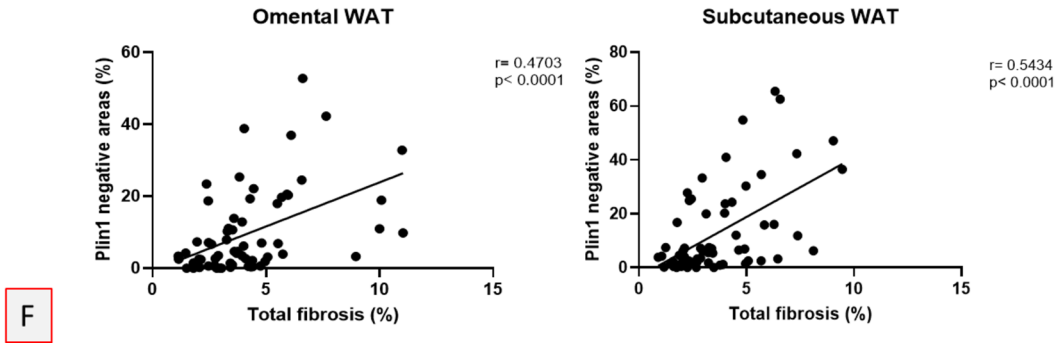

We then sought aimed to reproduce in vitro an adipocyte condition resembling that observed in obese adipose tissue. Fatty acids were added to the culture medium to induce adipocyte hypertrophy and generate hypertrophic adipocytes (HA)[39]. The mean size of lipid droplets was measured (Fig. 3B), and collagen gene expression in these cells was assessed (Fig. 3A). All three collagen types were expressed in hypertrophic-like adipocytes, with *COL3A1* markedly upregulated relative to fibroblasts. *COL6A3* expression, by contrast, was reduced in hypertrophic adipocytes compared with normal mature adipocytes, in line with data obtained in vivo from fat biopsies (see below).

Taken together, these findings further suggest that hypertrophic adipocytes may contribute to collagen fibril production and adipose tissue fibrosis.

◀**Fig. 1**. Fibrosis in human adipose tissue. **A**: Light and electron microscopy. Sirius Red staining (left and middle panels): representative images of fibrosis in visceral (omental) fat. In the right panel pericellular fibrosis is shown by high-resolution scanning electron microscopy (HRSEM, see Methods); scale bars: 50 µm (left), 15 µm (middle) and 7 µm (right). **B**: Fibrosis is significantly increased only in omental fat when compared with lean controls. **C**: Perilipin1 (PLIN1) immunohistochemistry. PLIN1-negative adipocytes (*) located near PLIN1-immunoreactive adipocytes are visible in a visceral biopsy from a patient with obesity; scale bar 40 µm. **D**: The percentage of PLIN1-negative parenchymal areas was higher in both subcutaneous and omental fat from patients with obesity. **E**: Correlation between PLIN1-negative parenchymal areas of visceral and subcutaneous fat in each patient. **F**: Correlation between the percentage of PLIN1-negative parenchymal areas and total fibrosis in subcutaneous and omental fat. Box-and-whisker plots with median and min-max values (**B** and **D**) represent the data distribution. Statistical significance was assessed by two-way ANOVA followed by the Benjamini– Yekutieli post hoc test. $^{**}p < 0.01$, $^{***}p < 0.001$.

	Fibrosis in oWAT		*Fibrosis in scWAT*	
	R	***P***	***R***	***P***
Age	**-0.16**	**0.25 (ns)**	**0.2**	**0.16 (ns)**
BMI	-0.12	0.39 (ns)	-0.03	0.83 (ns)
Adipocyte size (µm²)	-0.33	0.022	-0.35	0.01
Triglycerides	-0.37	0.02	-0.18	0.24 (ns)
HDL cholesterol	0.36	0.02	0.11	0.48 (ns)
Glycemia	-0.27	0.06 (ns)	-0.04	0.77 (ns)
HbA1c	-0.16	0.38 (ns)	0.04	0.84 (ns)

Table 1. Correlation analysis between adipose tissue fibrosis and clinical parameters.

Increased intra-abdominal pressure as a potential stimulus for visceral fat fibrosis

Next, we investigated what stimulus might drive collagen production in hypertrophic adipocytes. Adipocytes are known to be mechanosensitive and mechanoresponsive[40]. We considered mechanical pressure as a potential trigger because adipose tissue exposed to strong mechanical loading, such as plantar calcaneal fat, exhibits a distinctive architecture characterized by abundant pericellular collagen[41], a feature also observed in our samples (Suppl. Figure 3). We therefore investigated whether intra-abdominal pressure, which primarily affects visceral fat, is increased in patients with obesity. As previously reported[42], intra-abdominal pressure was elevated in individuals with obesity and positively correlated with abdominal circumference, a marker of visceral obesity (Suppl. Figure 4). These findings raise the possibility that increased mechanical pressure on adipocytes may trigger molecular mechanisms leading to increased collagen production and subsequent fibrosis.

Adipose tissue in obesity is inflamed

Adipocyte death[27] can promote fat inflammation, particularly in visceral fat[26,29], and inflammation has been implicated in the development of fibrosis[10]. We therefore assessed the presence of inflammatory cells. CD68 immunohistochemistry showed that the vast majority of inflammatory cells in both visceral and subcutaneous obese fat were macrophages, which are known to play an important role in triggering fibrosis[10,43]. Both tissues showed clear evidence of inflammation, with a positive correlation between macrophage abundance in visceral and subcutaneous fat within individual patients, and a higher macrophage density in visceral than in subcutaneous fat (Fig. 3C and Suppl. Figure 5 A).

Given the well-established pro-fibrotic activity of macrophages[10,43], we then examined the relationship between macrophage accumulation and fibrosis. A positive correlation was observed between macrophage density in fibrotic areas and the extent of fibrosis (Fig. 3D).

Since more than 90% of macrophages in obese mice are organized into crown-like structures (CLS)[27], we examined their spatial distribution in inflamed adipose tissues. Only a minority of macrophages were organized into CLS. Most were distributed among apparently normal adipocytes within the adipose parenchyma, although a substantial proportion was located within fibrotic areas, consistent with the correlations described above, or near vascular structures (Suppl. Figure 5B).

Overall, these data suggest that inflammation contributes to the development of adipose tissue fibrosis, consistent with previous reports[10,19,44].

Molecular mechanisms: role of collagen VI

While increased expression of collagens I and III in obese human adipose tissue has been consistently reported[30,31], data on collagen VI remain controversial[11–14].

Gene expression analyses in our patients revealed that obese visceral fat showed a significant decrease in *COL6A3* expression, whereas *COL1A1* and *COL3A1* levels were slightly increased (*COL1A1* by 23% and *COL3A1* by 30.7%) (Fig. 3E). We also observed a reciprocal relationship between BMI and fibrosis (positive correlation) and between BMI and *COL6A3* expression (negative trend) (Fig. 3F).

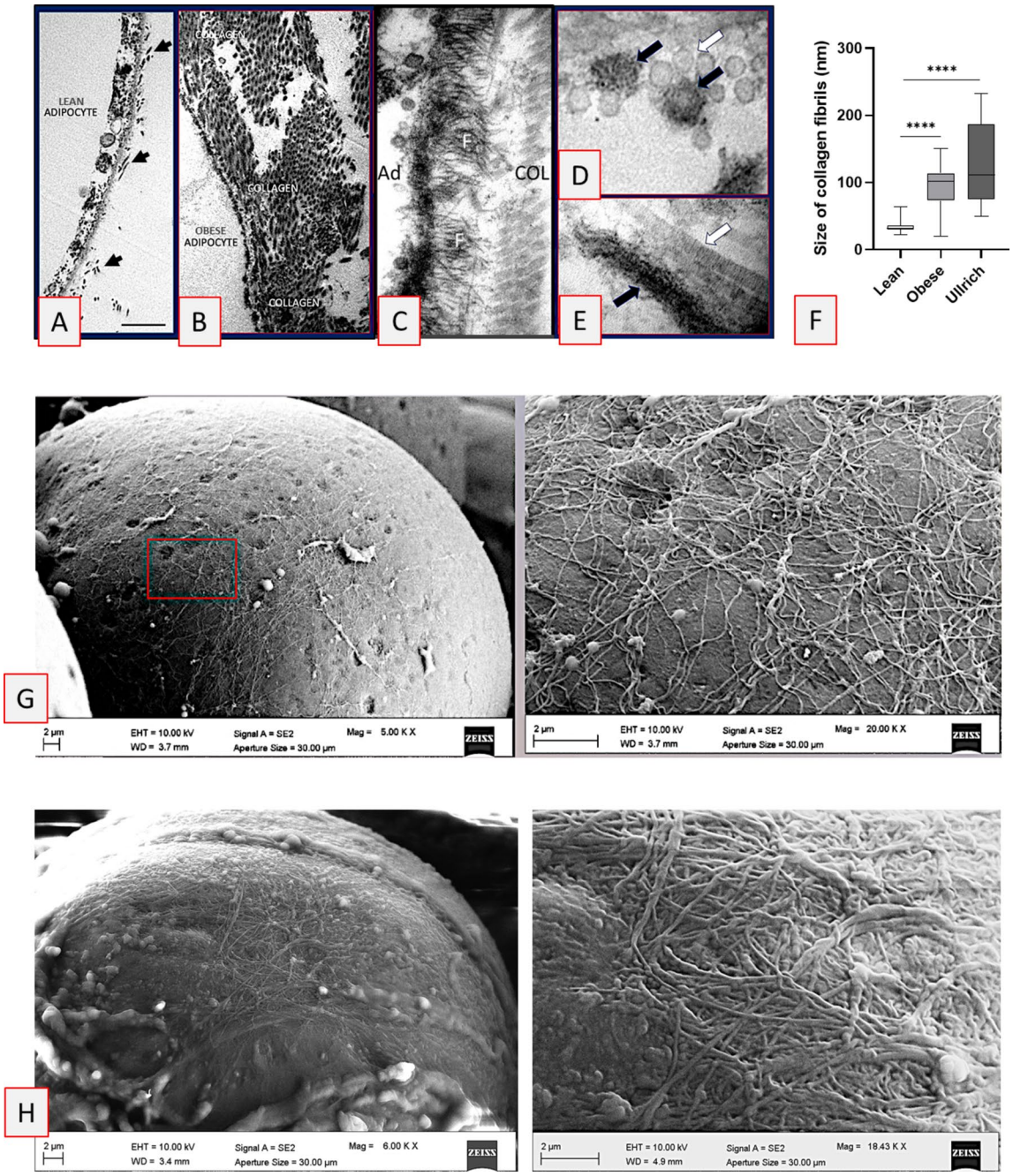

Fig. 2. Transmission (TEM) and high-resolution scanning (HRSM) electron microscopy of human visceral (omental) fat. **A**: TEM image from a lean control showing sparse collagen fibrils in close contact with the external adipocyte surface (arrows). **B**: TEM image from a representative biopsy from a patient with obesity showing abundant collagen fibrils tightly associated with the adipocyte surface. **C**: Representative image of a hypertrophic adipocyte (Ad) from obese fat showing microfibrils (F; possibly tropocollagen) apparently sprouting directly from the cell surface. COL: collagen fibrils. **D**: High-magnification transverse section of collagen fibrils shown in B, including enlarged dense fibrils (black arrows) compared with normal-like fibrils (white arrow). **E**: Longitudinal section of collagen fibrils showing altered fibril morphology (black arrow) compared with normal-like fibrils (white arrow). Scale bars: 1.2 µm in **A** and **B**, 280 nm in **C**, 100 nm in **D** and **E**. **F**: Size of collagen fibrils in lean, with obesity and fibrosis > 5% and Ullrich patients (see also 2.8 section of Results). **G**: Representative HRSEM images of omental fat from a lean patient (**G**) and a patient with obesity and fibrosis > 5% (**H**). Right panels show enlarged views of the boxed areas in the left panels. The fibrillar network surrounding adipocytes in adipose tissue from the patient with obesity shows increased fibril density and thickness. Scale bars as indicated. Box-and-whisker plots with median and min-max values (**F**) represent the data distribution. Statistical significance was assessed by Kruskal-Wallis test followed by Dunn's post hoc test. $^{****}p < 0.0001$.

We therefore investigated whether silencing *COL6A3* in hMADS affected *COL1A1* and *COL3A1* expression. After 7 days in culture, hMADS cells with approximately 50% *COL6A3* silencing showed increased expression of both genes, with *COL1A1* increasing by 75% and *COL3A1* by approximately 30% (Fig. 3G).

Patients with mutations in *COL6A2* and *COL6A3* genes

To determine whether collagen VI plays a role in adipose tissue fibrosis, as suggested by the findings described above, we analyzed subcutaneous adipose tissue from three patients with COL6-related myopathies (COL6-RMs): one patient with a homozygous *COL6A2* mutation and Ullrich congenital muscular dystrophy (UCMD), and two patients with Bethlem myopathy (BM) caused by heterozygous mutations in *COL6A2* (BM patient 1) and *COL6A3* (BM patient 2).

All three patients were lean according to BMI (clinical data in Table 2), and adipocyte size (mean area) was within the normal range when age was taken into account[45]: approximately 1,900μm^2 in the Ullrich patient (11 years old), about 4,590μm^2 in BM patient 1 (40 years old), and 3,870 μm^2 in BM patient 2 (41 years old), with a mean of 4,200 ± 360μm^2 compared with approximately 4,700 μm^2 in lean control subjects (no significant difference).

In all patients, we found a marked degree of fibrosis, quantified by Sirius Red staining of collagen fibers in adipose parenchyma using the same method applied for patients with obesity (see Methods). Fibrosis was most pronounced in the Ullrich patient (16.6% of parenchymal fat), followed by the Bethlem patients (6.7% BM patient 1 and 8.2% BM patient 2); all values were substantially higher than that observed in lean control subjects (2.5%) (Fig. 4A).

PLIN1 immunoreactivity revealed 5% of PLIN1-negative adipocytes in the Ullrich case and approximately 7% (patient 1) and 7.9% (patient 2) in the Bethlem cases (data not shown). Thus, despite the high level of fibrosis, the proportion of PLIN1-negative adipocytes was lower than that observed in obese fat (approximately 15%); this difference may reflect the smaller size of adipocytes in these patients (see above). CD68 immunostaining and TEM excluded significant signs of inflammation in all three patients (data not shown). In all cases, TEM showed a close association between adipocytes and collagen fibrils which, together with hypertrophy of organelles involved in protein synthesis and secretion, strongly suggests a direct contribution of these cells to collagen production (Fig. 4B left panel). Notably, in the Ullrich patient, altered enlarged fibrils resembling those observed in obese fat fibrosis were detected (Fig. 4B right panels, and Suppl. Figure 6), further suggesting that collagen VI plays an important role in collagen fibril production and stabilization, as proposed in previous studies[46]. Furthermore, considering that patients with obesity in this case series showed reduced expression of *COL6A3*, corresponding to the alteration observed in BM patient 2, we also examined *COL6A2* expression, corresponding to the alteration found in the Ullrich patient and BM patient 1, and found an approximately 15% reduction (Fig. 4C). Together, these data highlight the significant role collagen VI itself plays in adipocyte-driven fibrosis.

Role of CD38

Recent studies have reported significantly higher CD38 expression in the skin of subjects with systemic sclerosis than in healthy controls[20], suggesting that the CD38 ectoenzyme may play a key role in the onset of tissue fibrosis. We therefore investigated whether CD38 is also expressed in adipose tissues from patients with obesity.

Immunohistochemical analysis of omental (n = 8) and subcutaneous (n = 2) adipose tissue from obese patients, as well as omental (n = 3) and subcutaneous (n = 3) adipose tissue from lean patients, revealed occasional CD38-positive adipocytes and macrophages in lean subjects, in both subcutaneous and visceral fat. The positive adipocytes displayed a distinct granular-like morphology, suggesting intracytoplasmic localization of CD38[47]. Interestingly, a fibrotic area containing several fibroblast-like cells, which are widely considered to be responsible for fibrosis, was negative for CD38 in a subcutaneous biopsy (Fig. 5A left panels).

In the adipose tissues of patients with obesity, both adipocytes and macrophages in subcutaneous and visceral fat were frequently strongly positive for CD38. In particular, immunoreactivity in obese adipocytes showed a granular pattern. Fibrotic areas were also negative in these patients (Fig. 5A, right panels). A positive correlation between *CD38* gene expression and fibrosis was detected (Fig. 5B).

Taken together, these data indicate the overexpression of CD38 in both macrophages and adipocytes in the adipose tissue of individuals with obesity. We therefore investigated whether the human adipose cell line hMADS also expressed *CD38* and whether adipocyte hypertrophy was accompanied by increased expression. Our data showed that hMADS cells express *CD38*, and its expression increases in the hypertrophic adipocyte model (HA) (Fig. 5C).

Thus, in addition to collagen VI, CD38 may also play a role in human fat fibrosis. Using mature hMADS, we examined whether a functional relationship exists between *CD38* expression and *COL6A2* or *COL6A3* expression. The data showed that expression of *COL6* genes did not change following administration of a *CD38* stimulator (Suppl. Figures 7 and 8).

Taken together, these data support independent roles for collagen VI and CD38 in fat fibrosis.

Additional contributors to adipose tissue fibrosis

Data from other studies suggest that the cells responsible for fibrosis in obese human fat are myofibroblasts and adipocyte precursors[3,10,19]. Exploring whether a correlation exists between our data on fibrosis and markers of these cell types, we found a positive correlation with the myofibroblast marker *ASMA* (*ACTA2*), but not with *activin A* (*INHBA*) (Fig. 6A and B), a marker of adipocyte precursors[48]. This finding is consistent with the notion that myofibroblasts are central drivers of pathological fibrosis in adipose tissue, as they actively secrete and remodel extracellular matrix (ECM) components, contributing to the stiffening of the adipose microenvironment[49,50].

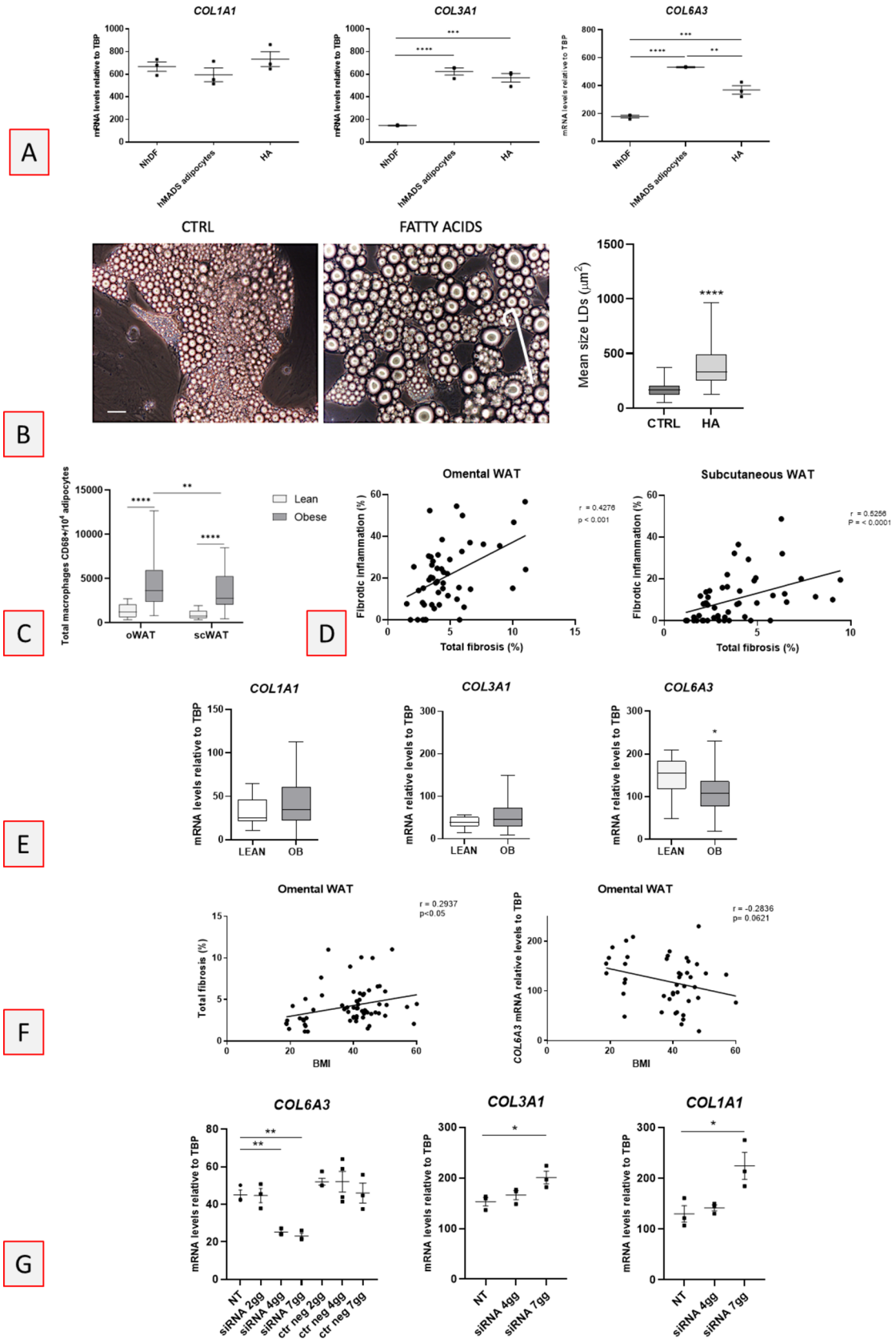

A negative correlation was found with the preadipocyte marker *PREF1* and a negative trend was observed for *PDGRA* (Fig. 6C and D), in line with the absence of a correlation with *INHBA* described above. The negative correlation observed with *PREF1* (preadipocyte factor) and the negative trend with *PDGFRA* suggest that fibrosis may damage adipogenesis by reducing the pool of functional preadipocytes. A fibrotic microenvironment, enriched in collagen and other ECM proteins, can impair adipocyte differentiation, reflecting an inverse

◀**Fig. 3**. Expression of collagen genes and inflammatory markers. **A**: In vitro gene expression of *COL1A1*, *COL3A1*, and *COL6A3* in a human adipocyte cell line (hMADS) and in human dermal fibroblasts (NhDF). Mature adipocytes express *COL1A1* at levels comparable to those of fibroblasts, but higher levels of *COL3A1* and *COL6A3* than NhDF cells. Hypertrophic adipocytes (HA), compared with mature adipocytes, express higher levels of *COL1A1* (ns) and lower levels of *COL6A3*. **B**: Light microscopy of differentiated hMADS. Addition of fatty acids to the medium induced hypertrophy of lipid droplets (LDs), mimicking the phenotype of hypertrophic obese adipocytes (HA) (left and middle panels). The mean size of LDs was significantly increased in differentiated hypertrophic hMADS cells (right panel). Scale bar: 10 µm. **C**: Quantitative data showing that CD68-immunoreactive macrophages are more abundant in both subcutaneous and visceral (omental) fat from patients with obesity. **D**: Positive correlations between the extent of fibrosis and the density of CD68-immunoreactive macrophages in fibrotic areas were observed in both visceral and subcutaneous fat. **E**: Increased expression of type I (*COL1A1*) and type III (*COL3A1*) collagen genes and reduced expression of *COL6A3* were observed in visceral adipose tissue from patients with obesity and lean controls. **F**: Omental (visceral) fat: positive correlation between BMI and fibrosis (left), and negative correlation between BMI and *COL6A3* (right). Data from lean individuals are included. **G**: hMADS with 48% silencing of *COL6A3* show increased production of *COL1A1* and *COL3A1* after 7 days. Aligned dot blots with mean ± S.E.M. (**A** and **G**) and box-and-whisker plots with median and min-max values (**B**, **C** and **E**) represent the data distribution. Statistical significance was assessed by one-way ANOVA with Tukey's HSD post-hoc test (**A**), unpaired two-tailed Student's t-test (**B**), two-way ANOVA followed by Benjamini– Yekutieli post hoc test (**C**), Mann-Whitney test (**E**), and either unpaired two-tailed Student's t-test or one-way ANOVA test with Tukey's HSD post hoc test (**G**). $^{*}p < 0.05$, $^{**}p < 0.01$, $^{***}p < 0.01$, $^{****}p < 0.0001$.

Patient	BMI	Phenotype	Onset	Age at first visit (yr)	Age at last visit (yr)	CK	First steps, months	Lost walk (age, yr)	NIV Age	%FVC	Mutation
1	17.8	BM	B	34	40	3	12	31	-	63	h *COL6A2* c.847G > A
2	17.4	UCMD	B	5	11	< 1	NW	-	4	29	H *COL6A2* c. 2572 C > T
3	21.7	BM	B	11	41	1.5	36	-	-	52	h *COL6A3* c. 6158G > T

Table 2. Clinical data of Ullrich and Bethlem patients. BM= Bethlem myopathy; UCMD= Ullrich congenital muscular dystrophy, B= birth; CK= creatine kinase (times upper value of normal); NW= never walked; NIV= nasal intermittent ventilation; %FVC= percent predicted forced vital capacity; h=heterozigous; H= homozygous. Age at last visit = age of biopsy.

relationship between fibrotic burden and the capacity of adipose progenitors to undergo healthy adipogenesis[51]. Autotaxin (ATX), also known as ectonucleotide pyrophosphatase/phosphodiesterase encoded by the *ENPP2* gene, has been suggested to play a role[52], but we found a negative correlation in our study (Fig. 6E). This negative correlation may reflect the complex, context-dependent role of lysophosphatidic acid (LPA) signaling in tissue remodeling. Moreover, we examined the correlation between extracellular peptidase D (*PEPD*) and fibrosis and found a negative correlation tendency in the visceral fat of our case series (Fig. 6F). This supports the idea that PEPD, which is responsible for collagen degradation and protection against a fibrotic microenvironment, plays a role in fibrosis, as suggested by previous studies[24]. Reduced expression or activity of PEPD may impair collagen remodeling, thereby facilitating the progression of fibrotic processes.

Discussion

Inflammation and fibrosis are the main histopathologic findings of human obese adipose tissue[2,3]. While the cause of inflammation has been clarified[26–29,53], the pathogenesis of fibrosis remains incompletely understood[30,31]. Data from our study support a role for three new additional possible actors: collagen VI, CD38, and the activity of hypertrophic adipocytes.

Three very rare patients with gene mutations causing reduced or absent collagen VI production showed intense fibrosis in their adipose tissue. Similarly, our data, partially in agreement with data from previous studies[11,14], show reduced expression of *COL6* genes in adipose tissue from patients with obesity and increased production of fibrillar collagen by mature human adipocytes in vitro after silencing of *COL6* genes.

Collagen VI is not a fibrillar collagen, and previous studies have shown that it localizes among collagen fibrils and contributes to their stabilization[11,18,46].

The mechanism is not clear, however, it has been established that, by interacting with both cellular receptors and ECM (extracellular matrix) components, collagen VI network regulates cellular functions and ECM organization, including collagen fibrillogenesis. Specifically, in adipose tissue, collagen VI is critical for the stability of tissue architecture[11].

Therefore, its role may relate to the containment function of the fibrillar network surrounding each adipocyte (Fig. 2). In this context, collagen VI could act as a glue-like component that enhances the mechanical resistance of the fibrillar network. Furthermore, this stable network of collagen fibrils may, through a feedback mechanism, inhibit the production of additional fibrils. This is consistent with observations that the absence or reduction of

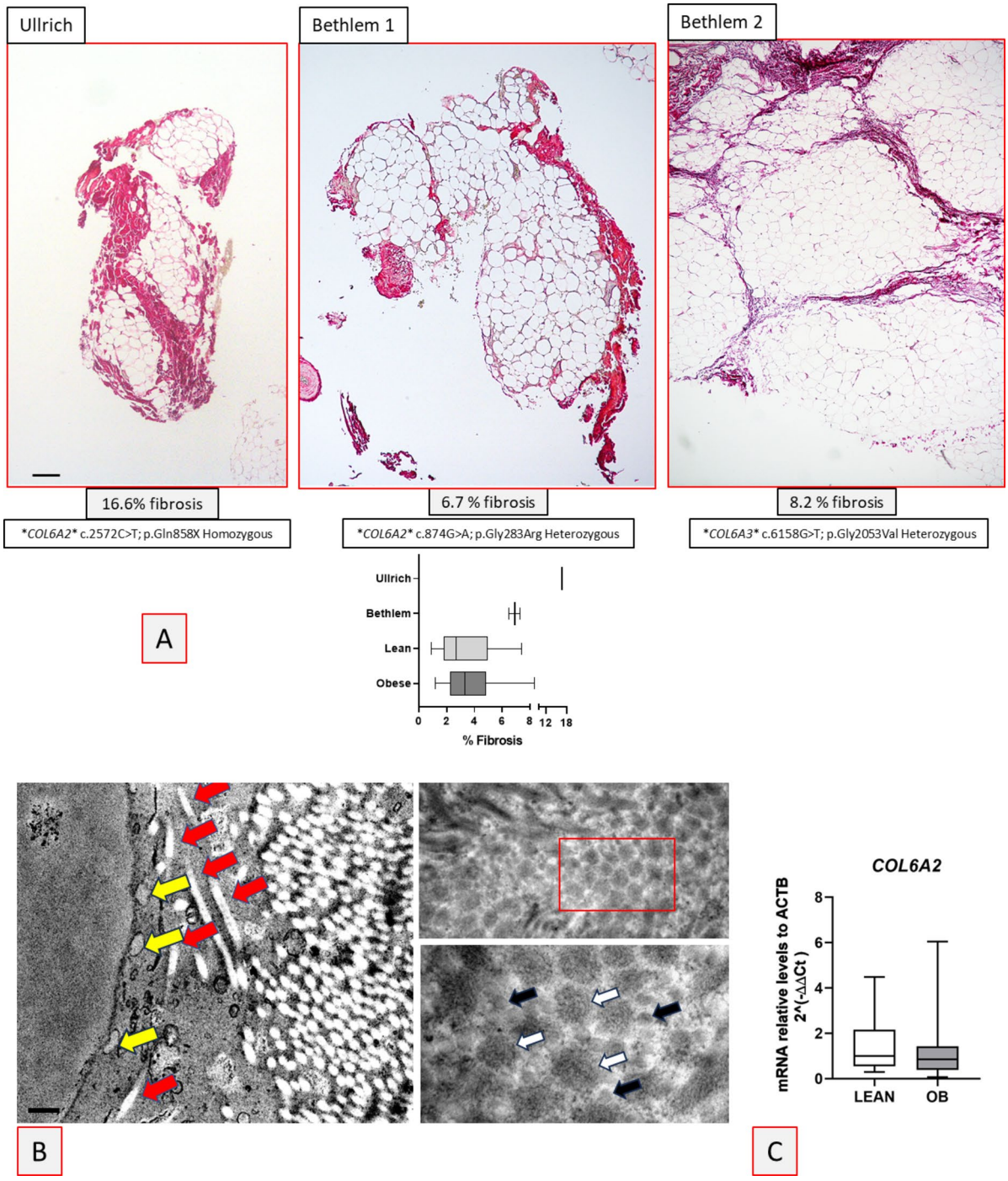

Fig. 4. Congenital mutations in human *COL6* genes in vivo appear to promote fibrillar collagen production by adipocytes. **A**: Representative light-microscopy images with Sirius Red staining of fat biopsies from the Ullrich case (left panel) and the Bethlem cases (middle and right panels). Details of the *COL6* gene mutations are indicated. Abundant lobular and pericellular fibrosis is evident in all cases. Scale bars: 80 µm (left panel), 45 µm (middle panel), and 50 µm (right panel). The graph summarizes the percentage of fibrosis detected in subcutaneous fat from the patients studied. **B**: Representative transmission electron microscopy (TEM) image from the Ullrich case showing abundant fibrillar collagen in close contact with a mature adipocyte (see also Suppl. Figure 6). Some mature collagen fibrils (red arrows) are visible within the cytoplasm (left panel). The lumen of the rough endoplasmic reticulum appears dilated (yellow arrows). The right panels show transverse sections of collagen fibrils. In the upper right panel, some collagen fibrils appear enlarged. The lower right panel shows a higher-magnification view of the boxed area in right upper panel. Enlarged fibrils (white arrows, some indicated) can be compared with normal fibrils (black arrows, some indicated) Scale bars: 200 nm in the left panel, 450 nm in the upper right panel, and 230 nm in the lower right panel. **C**: *COL6A2* expression tended to be lower in visceral fat from patients with obesity than in lean controls. Box-and-whisker plots with median and min-max values (**A** and **C**) represent the data distribution. Statistical significance was assessed by the Mann-Whitney test (**C**).

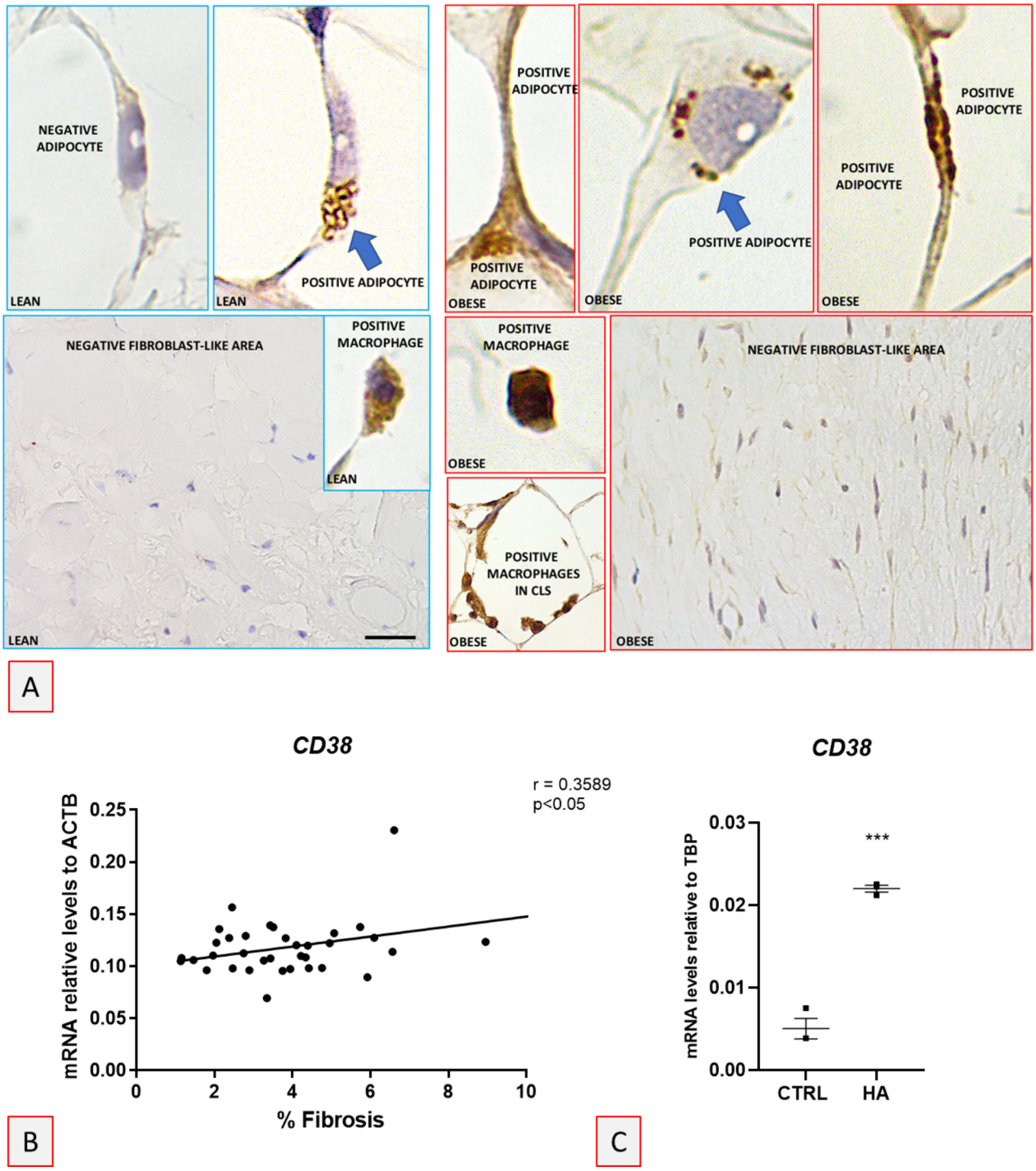

Fig. 5. CD 38 immunohistochemistry and in vivo and in vitro data. **A**: Light microscopy. Representative images from lean (LEAN) and obese (OBESE) visceral fat. Most lean adipocytes were negative. Rare positive adipocytes showed a granular-like positivity (arrow). Weakly positive macrophages were also found in lean fat. Fibrous tissue was negative in both lean and obese fat. Intense granular-like positivity was observed in adipocytes from patients with obesity. Macrophages were intensely positive both when located in interstitial parenchymal tissue and when forming CLS in obese fat. Scale bars: 3 µm in all upper panels; 30 µm in the lower left and right panels; 10 µm in the upper middle panels (macrophages), 30 µm in the lower middle panel (CLS). **B**: A positive correlation was found between fibrosis and CD38 gene expression. **C**: CD38 gene expression in the human adipocyte cell line hMADS under standard conditions and after the addition of fatty acids to the culture medium to obtain hypertrophic adipocytes (see also Fig. 3). Aligned dot blot with mean ± S.E.M. (**C**) represents the data distribution. Statistical significance was assessed by unpaired two-tailed Student's t-test (**C**). ***$p < 0.001$.

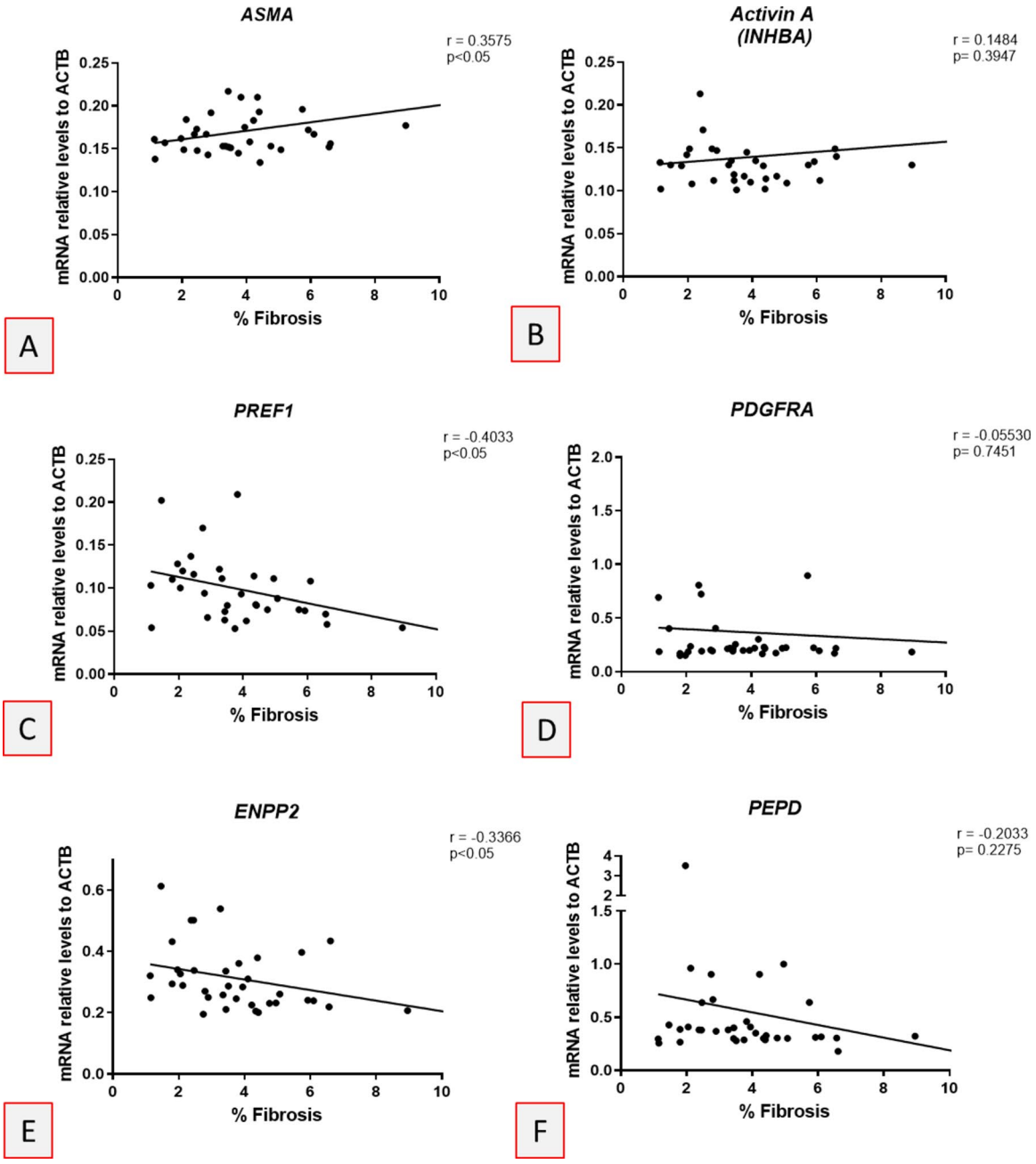

Fig. 6. Gene expression in visceral (omental) fat from patients with obesity in our case series. Correlations suggesting a role for myofibroblasts (*ASMA* with a positive tendency for *Activin A*) and peptidase D (*PEPD*) in the pathogenesis of visceral fat fibrosis were found (A, B and F). The data did not support a role for preadipocytes (*PDGFRA* and *PREF1*) or *ENPP2* (C, D and E).

COL6 gene function in the three rare cases described here is associated with markedly increased collagen fibril production and fibrosis in adipose tissue. Notably, leptin inhibits *COL6* expression[14]. *COL6* is regulated by leptin in human adipose tissue and reduced in obesity, and leptin production by adipocytes is well known to increase with cell size[54]. Therefore, it is plausible that the physiological rise in leptin production accompanying the progressive enlargement of adipocytes during lipid storage may locally weaken the mechanical strength of the pericellular network, thereby facilitating cellular expansion. Although still speculative, this hypothesis provides a unifying framework to account for several observations, including the abundance of collagen VI in adipose tissue, the inhibitory effect of leptin on *COL6* expression, the role of collagen VI in regulating collagen fibril production by adipocytes (with humans carrying *COL6* loss-of-function mutations showing marked adipose tissue fibrosis), and the reduced expression of *COL6* in obese adipose tissue.

Data from mice lacking collagen VI did not reveal any association with fat fibrosis[11]. However, it is also known that the phenotype is milder than in the human disorder, and muscle fibrosis has been described in three different models of mice lacking collagen VI[55].

Pericellular fibrosis is physiologically present in calcaneal fat, where body weight pressure plays a role in the need for elastic properties in this anatomical component of the human foot. In line with this, intra-abdominal pressure in patients with obesity is increased (present paper and[42], and shows a positive correlation with abdominal circumference, a marker of visceral obesity[56]. Furthermore, these findings are supported by experimental evidence showing that mechanical pressure on adipocytes induces fibro-inflammation[41,57,58]. Thus, increased intra-abdominal pressure may inhibit *COL6* expression, leading to reduced stability of the fibrillar network and subsequent overproduction of collagens I and III, thereby contributing to fat fibrosis. In line, both TEM and HRSEM showed altered collagen fibrils in the pericellular adipose tissue of patients with obesity > 5% and in Ullrich patient (Fig. 2).

Obese adipose tissue contains stressed and dead adipocytes, which promote inflammation mainly sustained by macrophages[26–29]. Recent studies have highlighted the role of the ectoenzyme CD38 as a key inducer of systemic fibrosis[20], with macrophages playing a central role in the general scheme of pathogenetic events leading to fibrosis[21,59–61]. Our immunohistochemistry data support a direct role for macrophages in CD38 production. Both lean and obese adipose tissues, when containing fibroblast-like cells, showed CD38 negativity, despite strong immunoreactivity in macrophages, in agreement with data from other authors[62,63]. CD38 immunoreactivity was intense in both obese adipocytes and macrophages, which were also increased in number. Moreover, we observed a positive correlation between *CD38* expression and fibrosis levels. We also found *CD38* expression in mature adipocytes in vitro, with a significant increase under hypertrophic-like experimental conditions.

Taken together, these findings indicate that CD38 may play a role in visceral fat fibrosis.

Another important consequence of macrophage infiltration into obese visceral fat is the well-known induction of TGF-β by TNF-α, which is produced by macrophages[64]. TGF-β is mainly produced by cells of the immune system, including macrophages, and this factor, a major promoter of tissue fibrosis, is highly elevated in obese adipose tissue in both mice and humans[23].

To investigate the relationship between *CD38* and *COL6*, we tested their interaction in mature adipocytes in vitro but found no correlation. These data, together with the striking evidence of high levels of fat fibrosis in patients with mutations in *COL6* genes in the absence of any significant macrophage infiltration in adipose tissue, suggest that these two factors likely play independent roles in the pathogenesis of fat fibrosis, with *CD38* activity primarily attributed to macrophages and *COL6* to adipocytes.

The cell type responsible for collagen fibril production is generally thought to be the myofibroblast[3,20], in agreement with our finding of a positive correlation between *ASMA* and fat fibrosis. However, some data from the present study seem to suggest that hypertrophic adipocytes could also play a role.

Combined analyses of hypertrophic adipocytes by TEM and HRSEM, together with in vitro data showing that mature human adipocytes (hMADS), compared with human dermal fibroblasts (NhDF), express similar levels of *COL1*, but more than three times the level of *COL3*, with a tendency for increased expression under hypertrophic-like conditions, support the idea that hypertrophic adipocytes could be, at least in part, responsible for visceral fat fibrosis in patients with obesity. Furthermore, the presence of intracytoplasmic collagen fibrils in adipocytes from the Ullrich patient, who showed the highest levels of fat fibrosis (Fig. 4C and Suppl. Figure 6) further supports direct collagen production by adipocytes. The presence of intracytoplasmic fibrils in cells with high levels of collagen production is well-documented in a case of desmoid fibromatosis, in which several fibroblasts showed intracytoplasmic collagen fibrils[65]. In addition, this hypothesis seems in line with recent proteomics data showing that isolated visceral adipocytes from mice, under high-fat diet, adopt a fibroblast-like phenotype[66] and considering that hypertrophic adipocytes have an increased metabolism that could include the fibrillar production[36].

Hypoxia induces HIFα, which stimulates fibrosis[22], and treatment with the HIFα-selective inhibitor PX-478 has been shown to alleviate fibrosis, inflammation, and glucose intolerance[30]. Our data confirm higher levels of HIF1α in obese visceral fat (data not shown), suggesting that hypoxia could be favored by pericellular and perilobular fibrosis (a form of self-choking-induced hypoxia by adipocytes). The impressive percentage of PLIN1 immunonegative adipocytes (about 15%) and the strong correlation with fat fibrosis found in this study point to the relevance of this mechanism.

Other factors contributing to fat fibrosis, such as reduced peptidase activity responsible for collagen degradation[24], are also consistent with our findings of a negative correlative tendency for *PEPD*. Autotaxin, a secreted enzyme that generates LPA, a bioactive lipid that influences cellular signaling and function upon binding to G protein-coupled receptors, is produced and released by human adipocytes and upregulated in obesity. It has been proposed to play a role in fat fibrosis[67]. However, we did not observe any correlation between its gene expression and fat fibrosis in our case series study, although the high variability among patients could account for this difference.

Conclusions

We propose that a series of interacting feedback loops may play a significant role in this pathology: fat accumulation induces increased abdominal pressure, which may contribute to a reduction in *COL6* gene expression in adipocytes, thereby favoring the hyperproduction of fibrillar collagens (types I and III). This interpretation is supported by our in vivo and in vitro findings, as well as by data from patients with congenital homozygous and heterozygous *COL6* mutations. The resulting pericellular and lobular fibrosis could trigger cellular and tissue hypoxia, giving rise to a complex vicious cycle: adipocyte hypertrophy → increased IAP →reduced collagen VI →increased collagen I and collagen III →self-choking and death of adipocytes →hypoxia and inflammation (macrophage infiltration) →TGF-β →CD38 hyperproduction →further fibrosis.

These findings highlight potential molecular players in the pathology of obesity-related visceral fat fibrosis, particularly the roles of collagen VI in adipocytes and CD38 in inflammatory macrophages. Given that CD38-targeting antibodies are already in clinical use for other pathologies[68,69], these insights may have therapeutic implications for treating obesity-related fibrosis.

Patients and methods

Sex as a biological variable

In this study design, sex was not considered as a biological variable.

Patients

Over the past five years, we collected adipose tissue biopsies from the subcutaneous and omental fat of 50 individuals undergoing bariatric surgery for severe obesity (body mass index [BMI] ≥ 35 kg/m^2) at Marche Polytechnic University, Ancona ($n = 33$) and at the "G.B. Morgagni" Polyclinic-University of Catania ($n = 17$). The clinical characteristics of these patients are summarized in Suppl. Table 1. Fat biopsies from the same anatomical sites were also obtained from control subjects (CTRL, $n = 15$) (BMI ≤ 25 kg/m^2 with abdominal circumference within the normal range) undergoing cholecystectomy at the "G.B. Morgagni" Polyclinic-University of Catania (Suppl. Table 2).

Subcutaneous fat biopsies were also collected from individuals with Ullrich congenital muscular dystrophy (UCMD) ($n = 1$) and Bethlem myopathy (BM) ($n = 2$) at the Rizzoli Orthopedic Institute, Department of Biomedical and Neuromotor Sciences, University of Bologna. Their clinical and genetic data are presented in Table 2.

Additionally, subcutaneous calcaneal fat samples from four patients aged 27–47 years were collected at the University of Verona, Department of Neuroscience, Biomedicine and Movement Sciences, who were treated for retrocalcaneal exostosis.

Light microscopy

For morphological analysis by light microscopy, all omental and subcutaneous fat samples were fixed in 4% paraformaldehyde in 0.1 M phosphate buffer (pH 7.4) overnight at 4 ° C. The samples were then dehydrated through a series of alcohol solutions of increasing concentration, clarified in xylene, and embedded in paraffin blocks. Serial paraffin Sect. (3 µm thick) were cut from each adipose biopsy using a sliding microtome (Leica RM 2135, Leica Microsystem, Milan, Italy), mounted onto glass slides, and dried.

Histochemistry with morphometry

Fibrosis quantification was performed using Sirius Red staining[70].

Paraffin sections (3 µm thick) were dewaxed in xylene and rehydrated through sequential immersions in alcohol solutions of decreasing concentration. The sections were then incubated with Picro-Sirius Red dye for one hour at room temperature. After extensive washing in water to remove excess dye, the sections were contrasted with Hematoxylin for 2 min, rinsed, dehydrated, and mounted using Eukitt® Mounting Medium (Merk Life Science S.r.l., Milan, Italy). Images of Sirius Red-stained tissues were captured at 2.5x magnification, with an average of 20 images acquired per biopsy. Fibrosis was semi-automatically quantified using ImageJ software: images were converted to grayscale, the red-stained areas were selected using the threshold command, and the percentage of total fibrosis was calculated. Fibrosis was expressed as the ratio of the red-stained area (fibrotic) to the total tissue area examined.

Immunohistochemistry with morphometry

Paraffin Sect. (3 µm thick) were deparaffinized and rehydrated. Unmasking procedures, using citric acid at 96 °C for 20 min, were used for the immunohistochemical detection of CD68. Then, sections were reacted with 0.3% hydrogen peroxide solution in distilled water for 5 min to block endogenous peroxidase activity. After rinsing in PBS, sections were treated for 20 min with a 2% normal serum blocking solution in PBS to block non-specific binding of the secondary antibody. The sections were then incubated overnight at 4 °C with the following primary antibodies: polyclonal rabbit anti-perilipin 1 (ab3526) 1:800 in PBS (Abcam, Cambridge, England); monoclonal mouse anti-CD68 (M0814) 1:200 in PBS (Dako, Glostrup, Denmark) and monoclonal antibody murine anti-human CD38, clone IB4, IgG2a Class, 1:300 in PBS [71].

After rinsing in PBS, biotinylated secondary antibody was added (1:200 dilution in PBS for 30 min; Vector Laboratories, Burlingame, CA). Sections were rinsed again in PBS and incubated with Avidin-Biotin peroxidase complex (1:100 in PBS for 60 min; Vectastain ABC kit Vector Laboratories). Sections were rinsed in PBS several times and finally the substrate Sigma Fast 3,3-diaminobenzidine (Sigma–Aldrich, Vienna, Austria) was added for 3 min. After immunohistochemical staining, sections were counterstained with Hematoxylin, dehydrated in ethanol, cleared with xylene, and mounted with Eukitt® Mounting Medium (Merk Life Science S.r.l., Milan, Italy). Negative controls, in which the primary antibody was omitted, showed no staining.

Morphometric analyses were performed on tissue sections observed with a light microscope (Zeiss Axioscop 40) (Carl Zeiss GmbH, Jena, Germany) to measure adipocyte size, the immunoreactive areas composed of perilipin 1 (PLIN1)-positive (vital) adipocytes, and the inflammatory state. All images were captured with a Zeiss Axiocam 503 color digital camera.

Adipocyte size: images were captured at 10x magnification and the mean area of at least 200 PLIN1 immunoreactive adipocytes per biopsy was calculated using ImageJ software.

Viability of adipocytes: sections were captured at 2.5x magnification to acquire a number of images corresponding approximately to the full size of the tissue section. Using ImageJ software, the total adipose tissue

area composed of PLIN1-positive and PLIN1-negative adipocytes was measured. The percentage of PLIN1 negativity was then calculated for each sample.

Inflammatory state: quantification of CD68-positive cells was performed. Approximately 20 random fields per tissue section were captured at 20x magnification, and CD68-positive macrophages were counted using ImageJ software. Counts were normalized to 10^4 adipocytes. Macrophages were categorized based on their distribution in five tissue districts: around dead adipocytes (arranged in crown-like structures: CLS)[27]; within fibrotic areas; within the parenchyma; inside blood vessels (intravascular); near blood vessels (perivascular). For each patient, the percentage of CD68-positive macrophages in each district was calculated. Additionally, CLS density (number of CLS per 10^4 adipocytes) was determined.

Transmission electron microscopy (TEM)

Some of the biopsies (24 in total, 18 from patients with obesity and 6 from lean patients) were also used for electron microscopy studies. For ultrastructural analysis, biopsies were fragmented into pieces measuring approximately 1 mm^3. Small tissue fragments were fixed in 2% glutaraldehyde and 2% paraformaldehyde in 0.1 mol/L Phosphate Buffer (PB), pH 7.4 for 4 h at room temperature. Samples were then post-fixed in 1% osmium tetroxide in 0.1 mol/L PB (1 h at 4 °C), dehydrated through a graded acetone series, and embedded in a mixture of Epon-Araldite. For each sample, semi-thin sections were cut (1.5 µm thick), and stained with toluidine blue. Ultrathin Sect. (60 nm) were then obtained using an MT-X ultratome (RMC; Tucson, AZ), stained with lead citrate, and examined with a Philips CM 10 transmission electron microscope (Philips, Eindhoven, Netherlands) operating at 100 kV. For each patient, at least three different thin sections, selected based on semithin toluidine blue staining, were observed.

Quantitative data on fibril size were obtained through direct measurements during observations, with at least 40–50 measurements per sample with a soft imaging system GmbH (Muenster, Germany) coupled with a MegaView G2 TEM camera (Evident, Waltham, MA, U.S.), performed per sample at high magnification, corresponding to the magnification shown in Fig. 2.

High-resolution scanning electron microscopy (HRSEM)

Small fragments of omental ($n=6$) and subcutaneous ($n=6$) adipose tissue from 6 patients affected by obesity with fibrosis > 5% and from 3 lean subjects were fixed in 2% glutaraldehyde–paraformaldehyde overnight at 4 °C. Samples were post-fixed in 1% osmium tetroxide (OsO_4) in PB for 60 min at 4 °C, washed in PB, and dehydrated through increasing ethanol concentrations. Dehydration was completed by critical point drying, consisting of incubation in increasing concentrations of hexamethyldisilazane (HMDS), up to 100% HMDS. Samples were mounted on aluminum stubs using cell adhesive carbon disks and sputter-coated with gold particles prior to SEM observation with a FESEM ZEISS SUPRA 40 microscope (Carl Zeiss NTS GmbH, Oberkochen, Germany). This FESEM has a theoretical resolution of 2 nm when operating at 10 kV and with a working distance of 2 mm.

Quantitative data on fibril size were obtained by direct measurements during observations, with at least 40–50 measurements performed per sample at high magnification, corresponding to the magnification shown in Fig. 2.

Intra-abdominal pressure measurements

We prospectively collected data from adult male patients admitted for brain injury to a single ICU (Anesthesia and Intensive Care Unit, University Hospital "Azienda Ospedaliero-Universitaria delle Marche", Ancona, Italy). Exclusion criteria included recent abdominal surgery, pancreatitis, cirrhosis with ascites, peritonitis or other abdominal infections, intra-abdominal or retroperitoneal masses, abdominal bleeding, retroperitoneal hematoma, and mechanical ventilation with PEEP values higher than 10 cmH2O.

After verifying all inclusion and exclusion criteria, intra-abdominal pressure (IAP) was measured using the Foley manometer technique. The manometer was placed between the catheter and the drainage device and primed with 20 mL of sterile saline solution. The "0 mmHg" reference mark was aligned with the symphysis pubis, and the filter was elevated vertically above the patient to record the bladder pressure, considered a surrogate measure of intra-abdominal pressure. Measurements were performed within the first 24 h after ICU admission.

Demographic and anthropometric data were collected, and waist circumferences were measured using abdominal CT scans. Patients were categorized into two groups: those with abdominal (visceral) obesity (waist circumference > 102 cm, $n=12$) and those without (waist circumference < 102 cm, $n=12$). All data were anonymized and analyzed blindly.

Molecular biology

Human samples

Fat biopsies were also used for molecular studies. Each biopsy was snap-frozen in liquid nitrogen, stored at − 80 °C, and used for the determination of gene expression.

Cell culture and treatments

Human multipotent adipose-derived stem cells (hMADS), kindly provided by Prof. Christian Dani (Université Côte D'Azur, Nice, France) were cultured as described previously[37]. In brief, hMADS grown in low-glucose (1 g/L) proliferation medium (Dulbecco's Modified Eagle's Medium [DMEM]) (Pan-Biotech GmbH, Aidenbach, Germany) supplemented with 10% FBS (Pan-Biotech GmbH , Aidenbach, Germany) and 2.5 ng/ml hFGF-2 (human recombinant fibroblast growth factor, PeproTech, London, UK) were used between the 16th and the 19th passage. To induce adipose differentiation, they were seeded in proliferation medium on multi-well plates at a density of 4500 cells/cm^2. Upon reaching confluence, hFGF-2 was not replaced. The next day

(designated day 0), cells were incubated in an adipogenic medium (serum-free proliferation medium/Ham's F-12 medium) supplemented with: 10 µg/ml transferrin, 5 µg/ml insulin, 0.2 nM triiodothyronine, 100 µM 3-isobutyl-1-methylxanthine, 1 µM dexamethasone, and 100 nM rosiglitazone. Dexamethasone and 3-isobutyl-1-methylxanthine were discontinued from day 3, and rosiglitazone from day 9. Treatments and biological assays were carried out on differentiated hMADS from day 12 to day 15.

Afterward, hypertrophic-like cells were obtained by treating differentiated hMADS for 12 days with adipogenic medium supplemented with fatty acids i.e., 350 µM palmitate and 350 µM oleate (Sigma–Aldrich, Milan, Italy). This concentration reflects the pathological levels of fatty acids (200–375 µM) adipose cells of obese individuals are exposed to. Fatty acid mixtures were replenished every 3 days, and hypertrophic-like adipocytes were obtained by day 32 [39]. For morphometric analyses of lipid droplets (LDs), images were captured at 10x magnification and the mean area of at least 100 LDs in differentiated hMADS and in differentiated hypertrophic hMADS was calculated using ImageJ software.

We also used a human dermal fibroblast cell line, NhDF [38](Thermo Fischer Scientific, USA), cultured in DMEM with 10% FBS.

COL6A3 gene silencing and modulation of CD38 gene expression

For *COL6A3* gene silencing, Lipofectamine® RNAiMAX (Invitrogen, Carlsbad, USA) was used to transfect differentiated hMADS according to the manufacturer's reverse transfection protocol.

Briefly, siRNAs were diluted in OPTI-MEM medium (siRNA final concentration was 2 µM) with Lipofectamine. Differentiated hMADS were transfected with siRNA *COL6A3* (siRNA ID: s3317) for silencing, while control cells were transfected with non-targeting negative control siRNA (scramble sequence) (both from Thermo Fisher Scientific, USA). Cells were incubated for 4 or 7 days.

For modulation of *CD38* gene expression, hMADS, were incubated for 48 h with 1 µM trans-Retinoic Acid (Sigma-Aldrich, USA).

COL1A1, *COL3A1*, *COL6A3* gene expression, as well as *CD38* gene modulation were assessed by qRT- PCR.

qRT-PCR

Total RNA from fat biopsies or from hMADS was extracted with TRIZOL reagent (Invitrogen, Carlsbad, CA), purified, digested with ribonuclease-free deoxyribonuclease, and concentrated using the RNeasy Micro Kit (Qiagen, Milan, Italy) according to the manufacturer's instructions. RNA concentrations were quantified using Nanodrop 1000 (Thermo Fisher Scientific, USA). For determination of mRNA levels, 1 µg RNA was reverse transcribed with a High-Capacity cDNA RT Kit with RNase Inhibitor (Applied BioSystems, Foster City, CA) in a total volume of 20 µl. qRT-PCR on patients (OB n = 37, lean n = 12) and hMADS was performed using TaqMan Gene Expression Assays and Master Mix TaqMan (#4453320, Applied Biosystems). All probes were from Applied Biosystems (Suppl. Table 3).

Reactions were carried out in a Step One Plus Real-Time PCR system (Applied BioSystems) using 50 ng cDNA in a final reaction volume of 10 µl. The thermal cycle protocol included initial incubation at 95 °C for 10 min followed by 40 cycles of 95 °C for 15 s and 60 °C for 20 s. A control reaction without reverse transcriptase in the amplification mixture was performed for each sample to rule out genomic contamination. Samples not containing the template were included in all experiments as negative controls. TATA box-binding protein was used as an endogenous control to normalize gene expression. Each sample was analyzed in triplicate. Relative mRNA expression was determined using the ΔCt method ($2^{-\Delta Ct}$).

For other qRT-PCR analyses (OB n = 25, lean n = 12), a StepOne TM Real-Time PCR System and a Power SYBR™ Green PCR Master Mix (Applied Biosystems, Foster City, CA, USA) were used, according to the manufacturer's protocol and as previously reported [72,73]. Each sample was analyzed in triplicate and the average was normalized to human ACTB expression.

Primers were designed by the "Primers-BLAST" tool from NCBI (https://www.ncbi.nlm.nih.gov/tools/primer-blast accessed on June 2023); transcript forward and reverse primer sequences, annealing temperature and fragment size are reported in Suppl. Table 4.

Amplification conditions included a cycle at 95 °C for 10 min, followed by 40 cycles at 95 °C for 15 s and 55–59 °C for 1 min. As a negative control, reaction without cDNA was performed (no template control, NTC). The RNA expression level for each sample was calculated using ΔCt values, normalized versus ACTB and reported as $2^{-\Delta\Delta Ct}$.

Western blot analysis

For CD38 protein detection, cells were washed twice with PBS and lysed in 1× RIPA buffer (50 mM Tris–HCl, pH 7.5, 150 mM NaCl, 1% Nonidet P-40, 1% sodium deoxycholate and 0.1% SDS) supplemented with protease and phosphatase inhibitors (Complete tablets and PhosSTOP cocktail; Roche, Switzerland). Protein concentration was determined using the DC Protein Assay (Bio-Rad, California, USA) according to the manufacturer's instructions.

Equal amounts of protein (20 µg) were separated on 4–15% Mini-PROTEAN® TGX™ precast gels (10-well; Bio-Rad, California, USA) and transferred onto nitrocellulose membranes (Bio-Rad, California, USA). Membranes were blocked and incubated overnight at 4 °C with the indicated primary antibodies. After incubation with HRP-conjugated secondary antibodies, immunoreactive bands were visualized using Pierce ECL Western Blotting Substrate (Thermo Fisher Scientific, Massachusetts, USA) and detected with a UVITEC chemiluminescence imaging system (Cambridge, UK).

Densitometric analysis was performed using ImageJ software. Primary antibodies were used at the following dilutions: anti-CD38 (1:1,000; MA5-44435, Invitrogen, USA) and anti-GAPDH (1:2,000; sc-47724, Santa

Cruz Biotechnology, USA). Secondary antibodies were goat anti-rabbit IgG (H + L)–HRP (1:10,000; Vector Laboratories, USA) for CD38 and m-IgG Fc BP–HRP (1:5,000; Santa Cruz Biotechnology, USA) for GAPDH.

Statistics

All experimental data are presented as mean ± S.E.M. or min-max values. Comparisons between groups were performed using a non-parametric Mann–Whitney test or a Kruskal-Wallis test followed by Dunn's post hoc test, one-way analysis of variance (ANOVA) with post-hoc Tukey HSD test, or an unpaired two-tailed Student's t-test. For multiple groups, two-way ANOVA followed by Benjamini–Yekutieli post hoc test was used. Statistical information and statistical significance values are indicated in the figures and figure legends. Finally, Pearson correlation coefficients (r) and p-values were calculated to assess correlations between variables. Differences were considered significant at $p \leq 0.05$. All experiments were carried out at least in triplicate.

Study approval

The study was conducted in accordance with the Declaration of Helsinki and was approved by the following ethics committees: Ancona (CERM 26/11/2020 Prot n. 2020 – 385 and the study protocol for intra-abdominal pressure measurements -protocol n. 2021 – 166); Catania (Research Ethics Committee Catania2, Garibaldi Hospital, 21/05/2021 Prot n. 374/CE); and Bologna (11/05/2021, project identification code: CE 0007151). All patients provided written informed consent.

Regarding samples collected at Verona University, patients consented to the anonymous use of their tissues, which would otherwise have been discarded. The materials were enumerated to maintain consistency across the different centers in which they were collected, but the samples were completely anonymized, and no link remains between the material and the patient, in accordance with current regulations (https://english.ccmo.nl/investigators/legal-framework-for-medical-scientific-research/your-research-is-it-subject-to-the-wmo-or-not;[74,75].

Therefore, no additional ethical approval was required.

Data availability

All data presented are included in the text.

Received: 20 January 2026; Accepted: 17 April 2026
Published online: 28 April 2026

References

1. Giordano, A. et al. The Adipose Organ Is a Unitary Structure in Mice and Humans. *Biomedicines* **10**, 2275 (2022).
2. Vidal-Puig, A. Adipose tissue expandability, lipotoxicity and the metabolic syndrome. *Endocrinol. Nutr.* **60** (Suppl 1), 39–43 (2013).
3. Marcelin, G., Silveira, A. L. M., Martins, L. B., Ferreira, A. V. & Clément, K. Deciphering the cellular interplays underlying obesity-induced adipose tissue fibrosis. *J. Clin. Invest.* **129**, 4032–4040 (2019).
4. Guglielmi, V. et al. Omental adipose tissue fibrosis and insulin resistance in severe obesity. *Nutr. Diabetes*. **5**, e175 (2015).
5. Hasegawa, Y. et al. Repression of Adipose Tissue Fibrosis through a PRDM16-GTF2IRD1 Complex Improves Systemic Glucose Homeostasis. *Cell. Metab.* **27**, 180–194e6 (2018).
6. Brown, K. A. & Scherer, P. E. Update on Adipose Tissue and Cancer. *Endocr. Rev.* **44**, 961–974 (2023).
7. Sun, K., Li, X. & Scherer, P. E. Extracellular Matrix (ECM) and Fibrosis in Adipose Tissue: Overview and Perspectives. *Compr. Physiol.* **13**, 4387–4407 (2023).
8. Wynn, T. A. Common and unique mechanisms regulate fibrosis in various fibroproliferative diseases. *J. Clin. Invest.* **117**, 524–529 (2007).
9. Hao, M. et al. The pathogenesis of organ fibrosis: Focus on necroptosis. *Br. J. Pharmacol.* **180**, 2862–2879 (2023).
10. Datta, R., Podolsky, M. J. & Atabai, K. Fat fibrosis: friend or foe? *JCI Insight*. **3**, e122289. 122289 (2018).
11. Khan, T. et al. Metabolic dysregulation and adipose tissue fibrosis: role of collagen VI. *Mol. Cell. Biol.* **29**, 1575–1591 (2009).
12. Pasarica, M. et al. Adipose tissue collagen VI in obesity. *J. Clin. Endocrinol. Metab.* **94**, 5155–5162 (2009).
13. Dankel, S. N. et al. COL6A3 expression in adipocytes associates with insulin resistance and depends on PPARγ and adipocyte size. *Obes. (Silver Spring)*. **22**, 1807–1813 (2014).
14. McCulloch, L. J. et al. COL6A3 is regulated by leptin in human adipose tissue and reduced in obesity. *Endocrinology* **156**, 134–146 (2015).
15. Crewe, C., An, Y. A. & Scherer, P. E. The ominous triad of adipose tissue dysfunction: inflammation, fibrosis, and impaired angiogenesis. *J. Clin. Invest.* **127**, 74–82 (2017).
16. Merlini, L. et al. New Clinical and Immunofluoresence Data of Collagen VI-Related Myopathy: A Single Center Cohort of 69 Patients. *Int. J. Mol. Sci.* **24**, 12474 (2023).
17. Norwood, F. L. M. et al. Prevalence of genetic muscle disease in Northern England: in-depth analysis of a muscle clinic population. *Brain* **132**, 3175–3186 (2009).
18. DeBari, M. K. & Abbott, R. D. Adipose Tissue Fibrosis: Mechanisms, Models, and Importance. *Int. J. Mol. Sci.* **21**, 6030 (2020).
19. Marcelin, G., Gautier, E. L. & Clément, K. Adipose Tissue Fibrosis in Obesity: Etiology and Challenges. *Annu. Rev. Physiol.* **84**, 135–155 (2022).
20. Shi, B. et al. Targeting CD38-dependent NAD+ metabolism to mitigate multiple organ fibrosis. *iScience* **24**, 101902 (2021).
21. Avvedimento, E. V. & Gabrielli, A. Linking NAD metabolism and DNA repair to inflammation in SSc. *Nat. Rev. Rheumatol.* **17**, 381–382 (2021).
22. Halberg, N. et al. Hypoxia-inducible factor 1alpha induces fibrosis and insulin resistance in white adipose tissue. *Mol. Cell. Biol.* **29**, 4467–4483 (2009).
23. Yadav, H. et al. Protection from obesity and diabetes by blockade of TGF-β/Smad3 signaling. *Cell. Metab.* **14**, 67–79 (2011).
24. Pellegrinelli, V. et al. Dysregulation of macrophage PEPD in obesity determines adipose tissue fibro-inflammation and insulin resistance. *Nat. Metab.* **4**, 476–494 (2022).
25. Björntorp, P. Size, number and function of adipose tissue cells in human obesity. *Horm Metab. Res Suppl.* **4**, 77–83 (1974).
26. Camastra, S. et al. Muscle and adipose tissue morphology, insulin sensitivity and beta-cell function in diabetic and nondiabetic obese patients: effects of bariatric surgery. *Sci. Rep.* **7**, 9007 (2017).
27. Cinti, S. et al. Adipocyte death defines macrophage localization and function in adipose tissue of obese mice and humans. *J. Lipid Res.* **46**, 2347–2355 (2005).

28. Strissel, K. J. et al. Adipocyte death, adipose tissue remodeling, and obesity complications. *Diabetes* **56**, 2910–2918 (2007).
29. Murano, I. et al. Dead adipocytes, detected as crown-like structures, are prevalent in visceral fat depots of genetically obese mice. *J. Lipid Res.* **49**, 1562–1568 (2008).
30. Sun, K., Tordjman, J., Clément, K. & Scherer, P. E. Fibrosis and adipose tissue dysfunction. *Cell. Metab.* **18**, 470–477 (2013).
31. Divoux, A. et al. Fibrosis in human adipose tissue: composition, distribution, and link with lipid metabolism and fat mass loss. *Diabetes* **59**, 2817–2825 (2010).
32. Trayhurn, P. Hypoxia and adipose tissue function and dysfunction in obesity. *Physiol. Rev.* **93**, 1–21 (2013).
33. Lee, Y. S. et al. Increased adipocyte O2 consumption triggers HIF-1α, causing inflammation and insulin resistance in obesity. *Cell* **157**, 1339–1352 (2014).
34. Spalding, K. L. et al. Dynamics of fat cell turnover in humans. *Nature* **453**, 783–787 (2008).
35. Giordano, A. et al. Obese adipocytes show ultrastructural features of stressed cells and die of pyroptosis. *J. Lipid Res.* **54**, 2423–2436 (2013).
36. Ginzberg, M. B., Kafri, R. & Kirschner, M. Cell biology. On being the right (cell) size. *Science* **348**, 1245075 (2015).
37. Rodriguez, A. M. et al. Adipocyte differentiation of multipotent cells established from human adipose tissue. *Biochem. Biophys. Res. Commun.* **315**, 255–263 (2004).
38. Cometa, S. et al. Innovative Eco-Friendly Hydrogel Film for Berberine Delivery in Skin Applications. *Molecules* **26**, 4901 (2021).
39. Aprile, M. et al. In-Vitro-Generated Hypertrophic-Like Adipocytes Displaying PPARG Isoforms Unbalance Recapitulate Adipocyte Dysfunctions In Vivo. *Cells* **9**, 1284 (2020).
40. Yuan, Y., Gao, J. & Ogawa, R. Mechanobiology and Mechanotherapy of Adipose Tissue-Effect of Mechanical Force on Fat Tissue Engineering. *Plast. Reconstr. Surg. Glob Open.* **3**, e578 (2015).
41. Chanda, A. & McClain, S. Mechanical Modeling of Healthy and Diseased Calcaneal Fat Pad Surrogates. *Biomimetics (Basel).* **4**, 1 (2019).
42. Sugerman, H. J. Increased intra-abdominal pressure in obesity. *Int. J. Obes. Relat. Metab. Disord.* **22**, 1138 (1998).
43. Keophiphath, M. et al. Macrophage-secreted factors promote a profibrotic phenotype in human preadipocytes. *Mol. Endocrinol.* **23**, 11–24 (2009).
44. Gliniak, C. M., Pedersen, L. & Scherer, P. E. Adipose tissue fibrosis: the unwanted houseguest invited by obesity. *J. Endocrinol.* **259**, e230180 (2023).
45. Knittle, J. L., Timmers, K., Ginsberg-Fellner, F., Brown, R. E. & Katz, D. P. The growth of adipose tissue in children and adolescents. Cross-sectional and longitudinal studies of adipose cell number and size. *J. Clin. Invest.* **63**, 239–246 (1979).
46. Sabatelli, P., Merlini, L., Di Martino, A., Cenni, V. & Faldini, C. Early Morphological Changes of the Rectus Femoris Muscle and Deep Fascia in Ullrich Congenital Muscular Dystrophy. *Int. J. Environ. Res. Public. Health.* **19**, 1252 (2022).
47. Lee, H. C., Deng, Q. W. & Zhao, Y. J. The calcium signaling enzyme CD38 - a paradigm for membrane topology defining distinct protein functions. *Cell. Calcium.* **101**, 102514 (2022).
48. Zaragosi, L. E. et al. Activin A Plays a Critical Role in Proliferation and Differentiation of Human Adipose Progenitors. *Diabetes* **59**, 2513–2521 (2010).
49. Hinz, B. & Lagares, D. Evasion of apoptosis by myofibroblasts: a hallmark of fibrotic diseases. *Nat. Rev. Rheumatol.* **16**, 11–31 (2020).
50. Ban, J. Q., Ao, L. H., He, X., Zhao, H. & Li, J. Advances in macrophage-myofibroblast transformation in fibrotic diseases. *Front. Immunol.* **15**, 1461919 (2024).
51. Zhang, Q. et al. Challenges and opportunities in obesity: the role of adipocytes during tissue fibrosis. *Front. Endocrinol. (Lausanne).* **15**, 1365156 (2024).
52. Rancoule, C. et al. Pro-fibrotic activity of lysophosphatidic acid in adipose tissue: in vivo and in vitro evidence. *Biochim. Biophys. Acta.* **1841**, 88–96 (2014).
53. Luca, T., Pezzino, S., Puleo, S. & Castorina, S. Lesson on obesity and anatomy of adipose tissue: new models of study in the era of clinical and translational research. *J. Transl Med.* **22**, 764 (2024).
54. Friedman, J. M. Leptin and the endocrine control of energy balance. *Nat. Metab.* **1**, 754–764 (2019).
55. Lamandé, S. R., Bateman, J. F. & Collagen VI disorders: Insights on form and function in the extracellular matrix and beyond. *Matrix Biol.* **71–72**, 348–367 (2018).
56. Ross, R. et al. Waist circumference as a vital sign in clinical practice: a Consensus Statement from the IAS and ICCR Working Group on Visceral Obesity. *Nat. Rev. Endocrinol.* **16**, 177–189 (2020).
57. Pellegrinelli, V. et al. Human adipocyte function is impacted by mechanical cues. *J. Pathol.* **233**, 183–195 (2014).
58. Frosti, C. L., Connelly, S. P. & Layne, M. D. Mechanobiology of Adipose Tissue Remodeling. *Tissue Eng. Part. A.* https://doi.org/10.1177/19373341251405218 (2025).
59. Chini, C. C. S., Cordeiro, H. S. & Tran, N. L. K. Chini, E. N. NAD metabolism: Role in senescence regulation and aging. *Aging Cell.* **23**, e13920 (2024).
60. Yarbro, J. R., Emmons, R. S. & Pence, B. D. Macrophage Immunometabolism and Inflammaging: Roles of Mitochondrial Dysfunction, Cellular Senescence, CD38, and NAD. *Immunometabolism* 2, e200026 (2020).
61. Pezone, A. et al. Inflammation and DNA damage: cause, effect or both. *Nat. Rev. Rheumatol.* **19**, 200–211 (2023).
62. Fedele, G. et al. CD38 ligation in peripheral blood mononuclear cells of myeloma patients induces release of protumorigenic IL-6 and impaired secretion of IFNγ cytokines and proliferation. *Mediators Inflamm* 564687 (2013).
63. Frasca, L. et al. IFN-gamma arms human dendritic cells to perform multiple effector functions. *J. Immunol.* **180**, 1471–1481 (2008).
64. Samad, F., Yamamoto, K., Pandey, M. & Loskutoff, D. J. Elevated expression of transforming growth factor-beta in adipose tissue from obese mice. *Mol. Med.* **3**, 37–48 (1997).
65. Welsh, R. A. Intracytoplasmic collagen formations in desmoid fibromatosis. *Am. J. Pathol.* **49**, 515–535 (1966).
66. Jones, J. E. C. et al. The Adipocyte Acquires a Fibroblast-Like Transcriptional Signature in Response to a High Fat Diet. *Sci. Rep.* **10**, 2380 (2020).
67. Ferry, G. et al. Autotaxin is released from adipocytes, catalyzes lysophosphatidic acid synthesis, and activates preadipocyte proliferation. Up-regulated expression with adipocyte differentiation and obesity. *J. Biol. Chem.* **278**, 18162–18169 (2003).
68. Malavasi, F. et al. Evolution and function of the ADP ribosyl cyclase/CD38 gene family in physiology and pathology. *Physiol. Rev.* **88**, 841–886 (2008).
69. Horenstein, A. L. et al. Monoclonal anti-CD38 therapy in human myeloma: retrospects and prospects. *Front. Immunol.* **16**, 1519300 (2025).
70. Malkusch, W., Rehn, B. & Bruch, J. Advantages of Sirius Red staining for quantitative morphometric collagen measurements in lungs. *Exp. Lung Res.* **21**, 67–77 (1995).
71. Deaglio, S., Aydin, S., Vaisitti, T., Bergui, L. & Malavasi, F. CD38 at the junction between prognostic marker and therapeutic target. *Trends Mol. Med.* **14**, 210–218 (2008).
72. Scuderi, C. et al. Gain-Type Aneuploidies Influence the Burden of Selective Long Non-Coding Transcripts in Colorectal Cancer. *Int. J. Mol. Sci.* **25**, 5538 (2024).
73. Castorina, S. et al. Gastric ghrelin cells in obese patients are hyperactive. *Int. J. Obes. (Lond).* **45**, 184–194 (2021).
74. Blewett, C. From 'Consent or Anonymise' to 'Share and Protect': Facilitating Access to Surplus Tissue for Research Whilst Safeguarding Donor Interests. *Health Care Anal.* **29**, 213–230 (2021).

75. Remes Lenicov, F. & Fink, N. E. Ethical issues in the use of leftover samples and associated personal data obtained from diagnostic laboratories. *Clin. Chim. Acta*. **117442** https://doi.org/10.1016/j.cca.2023.117442 (2023).

Acknowledgements
We thank Prof Oriano Francescangeli of Department of Science and Engineering of Materials, Environment and Urban Planning, Marche Polytechnic University, Ancona for revision of the biomechanical aspects of the peri-adipocyte fibrillar network and Dr Laura McLean, Lecturer at University of Torino for revising the English version of the manuscript.

Author contributions
S.Ci. and S.Ca. planned, performed and analyzed experiments with the help of A.DV., T.L., J.P., V.B., M.T., S.P., C.S., A.DC., MV.N., N.F., F.CC., A.S., L.G., T.S., C.D., M.MB., D.F.C., A.Ga., F.M., A.Gi., G.L., V.DG., A.D., E.C., A.P., M.P., L.M., P.S., collected, interpreted and contributed clinical data.S.Ci. designed and supervised the study.A.Ga., A.Gi., F.M., L.M., P.S., L.G. and T.S., gave critical intellectual content.S.Ci. wrote the manuscript with the help of T.L., L.M., P.S., L.G., T.S. and A.Gi.A.DV and T.L. shared first authors. Regarding authorship order for first authors, it was based on the number of cases personally studied.S.Ci and S.Ca. shared last authors.

Funding
Italian Ministery of Research: PRIN 2017 to S.Ci. and A.G, grant number #2017L8Z2, and Foundation of Molecular Medicine and Cellular Therapy Marche Polytechnic University, Ancona, Italy. Pia.Ce.Ri research development plan to S.Ca., Department of Medical, Surgical Sciences and Advanced Technologies "GF Ingrassia" (DGFI) University of Catania, # 2020–2022 Catania, Italy. National Council for Scientific and Technological Development. (CNPq-Brazil) - (200295/2022-5) to F. C. C.

Declarations

Competing interests
The authors declare no competing interests.

Additional information
Supplementary Information The online version contains supplementary material available at https://doi.org/10.1038/s41598-026-49848-7.

Correspondence and requests for materials should be addressed to S.C.

Reprints and permissions information is available at www.nature.com/reprints.

Publisher's note Springer Nature remains neutral with regard to jurisdictional claims in published maps and institutional affiliations.